Numerical Heat Transfer, vol. 9, pp. 43–57, 1986

A UNIFIED MODEL OF RADIALLY SYMMETRIC HEAT CONDUCTION

T. V. Hromadka II
Water Resources Division, U.S. Geological Services, Laguna Niguel, California 92677

The nodal domain integration method is applied to a radially symmetric heat conduction problem where the solution domain is discretized into irregular radial finite elements, and the state variable is approximated by a spatial linear trial function within each finite element. The resulting finite-element model represents the well-known Galerkin finite-element, subdomain-integration, and an integrated finite-difference numerical statement as well as an infinity of other mass-lumped matrix schemes. From the NDI approach, the several numerical modeling techniques are unified into one global domain model where each submodel can be obtained by the specification of a single mass-lumping parameter.

INTRODUCTION

Hromadka and Guymon [1] recently developed a nodal domain integration (NDI) model of three-dimensional heat conduction based on a tetrahedral finite element. From this numerical model, the finite-difference, subdomain integration, Galerkin finite-element methods, and an infinity of finite-element mass-lumped matrix models are unified into a single numerical statement.

In this paper the NDI technique is applied to the one-dimensional, radial-coordinate finite element. It is shown that the Galerkin finite-element, subdomain-integration, and an integrated finite-difference numerical model, are obtained by the appropriate specification of a single parameter in the resulting NDI statement. Thus, all three numerical approaches are unified into one numerical statement similar in form to a Galerkin finite-element matrix system. The extension of the NDI technique to developing unified cylindrical and spherical coordinate models follows from the derived radial coordinate model and the referenced NDI three-dimensional tetrahedral finite-element model [1].

The purpose of this paper is threefold. The first objective is to present a basic description of the NDI technique as applied to the class of partial differential equations generally encountered in the theory of diffusion and heat conduction. Sufficient set definitions and integral manipulations are provided in order that the extensions of the results to cylindrical and spherical coordinate systems are direct. The theoretical foundations of this numerical technique are based on the subdomain version of the finite-element weighted-residuals approach and incorporate the mass-lumping techniques used in some finite-element approaches.

The second objective is to develop the NDI numerical statement that represents the finite-element Galerkin statement, subdomain integration numerical statement, and integrated finite-difference control-volume statement by the specification of a single parameter in the resulting radial-element matrix system.

NOMENCLATURE

$A(\phi)$	operator	W_j	weighting function
K	thermal conductivity	x,y	spatial coordinates
N_j	basis functions	w_j,y_j	nodal coordinates
$\mathbf{p}^e$	element mass matrix	Γ	boundary
$\mathbf{Q}^e$	element mass matrix (radial)	η	mass-lumping factor
r_i	radial coordinate of node i	ϕ	temperature
R_j	control volume j	$\hat{\phi}$	approximation of ϕ
R,t	radial and time coordinates	Ω	domain
S	capacitance	Ω^e	finite element e
S_e	set of nodes associated with finite element e	Ω_j^e	nodal domain associated with control volume j and finite element e
$\mathbf{S}^e$	element stiffness matrix		

A third objective is to use the unified NDI formulation to gain insight into the performance of the several well-known domain models in the approximation of radially symmetric heat conduction processes. Since the NDI model represents each of the most popular numerical models as point values of the NDI approximation statement, the same computer code can be used for each numerical analog, as well as an arbitrary finite-element mass-lumping scheme.

NODAL DOMAIN INTEGRATION MODEL DEVELOPMENT

The partial differential equation describing radially symmetric heat conduction in an isotropic homogeneous medium is given by

$$\frac{\partial}{\partial R}\left(RK\frac{\partial \phi}{\partial R}\right) = RS\frac{\partial \phi}{\partial t} \tag{1}$$

where K is the thermal conductivity; S is the heat capacity; R is the radial coordinate; ϕ is temperature; and t is time.

The finite-element technique approximately solves the governing equation on a finite-element discretization of the domain [2]. The integrated finite-difference method uses a control-volume discretization [3].

The nodal domain integration approach partitions a finite element into smaller "nodal domains" that are defined geometrically as the intersection of the finite elements and control volumes. The utility of this further partitioning of the finite element is that an integrated finite-difference or a subdomain integration analog can be conveniently written in terms of a matrix system similar to the Galerkin finite-element matrix system. Additionally, flux-type boundary conditions can be accommodated on the problem domain boundary without the need for special equations or finite-difference approximations. The following set definitions of subdomains (control volumes), finite elements, and nodal domains will be used to develop the NDI finite-element matrix system.

Consider the partial differential operator relationship

$$A(\phi) = f;\ (x, y) \in \Omega,\ \Omega = \Omega \cup \Gamma \tag{2}$$

defined on global domain Ω with boundary condition types of Dirichlet or Neumann specified on global boundary Γ. An n-nodal point distribution can be defined in Ω with arbitrary density such that an approximation $\hat{\phi}$ for ϕ is defined in Ω by

$$\hat{\phi} = \sum_{j=1}^{n} N_j(x, y)\phi_j; (x, y) \in \Omega \tag{3}$$

where $N_j(x, y)$ are linearly independent global shape functions and ϕ_j are assumed values of the state variable ϕ at nodal point j. In Eq. (3) it is assumed that except for a set of Lebesque measure zero

$$\lim_{n\to\infty} \hat{\phi} = \lim_{\max\|(x_j, y_j), (x_k, y_k)\|\to 0} \hat{\phi} = \phi, (x, y) \in \Omega \tag{4}$$

A closed connected spatial subset R_j is defined for each nodal point j such that

$$\Omega = \bigcup_{j=1}^{n} R_j \tag{5}$$

The sets R_j are generally called control volumes or subdomains and are usually accompanied by additional requirements that

$$(x_j, y_j) \in R_j; (x_j, y_j) \notin R_k, j \neq k \tag{6}$$

and

$$R_j = R_j \cup B_j \tag{7}$$

where (x_j, y_j) are the spatial coordinates of node j, and B_j is the boundary of R_j. It is assumed that every subdomain is disjoint except along shared boundaries, that is,

$$R_j \cap R_k = B_j \cap B_k \tag{8}$$

The subdomain method of the finite-element weighted-residuals approach approximates Eq. (2) by solving the n equations

$$\int_{\Omega} [A(\phi) - f]w_j \, dA = 0 \quad j = 1, 2, \ldots, n \tag{9}$$

where

$$w_j = \begin{cases} 1, (x, y) \in R_j \\ 0, (x, y) \notin R_j \end{cases} \tag{10}$$

A second cover of Ω is defined by the finite-element method with

$$\Omega = \cup\Omega^e \tag{11}$$

where Ω^e is the closure of finite-element domain Ω^e and its boundary Γ^e.

Let S_e be the set of subscripts defined by

$$S_e \equiv \{j | \Omega^e \cap R_j \neq \{\phi\}\} \tag{12}$$

that is, S_e is simply the set of nodes associated with Ω^e. Then a set of nodal domains Ω_j^e is defined for each finite-element domain Ω^e by (Fig. 1)

$$\Omega_j^e = \Omega^e \cap R_j \qquad j \in S_e \tag{13}$$

The subdomain method of weighted residuals as expressed by Eq. (9) can be rewritten in terms of the subdomain cover of Ω by

$$\int_\Omega [A(\phi) - f] w_j \, dA = \int_{R_j} [A(\phi) - f] \, dA \tag{14}$$

With respect to the finite-element discretization of Ω,

$$\int_{R_j} [A(\phi) - f] \, dA = \int_{R_j \cap \Omega^e} [A(\phi) - f] \, dA \tag{15}$$

where for each finite element Ω^e a matrix system is given by generating for each nodal point $j \in S_e$,

$$\int_{\Omega^e \cap R_j} [A(\phi) - f] \, dA = \int_{\Omega_j^e} [A(\phi) - f] \, dA \qquad j \in S_e \tag{16}$$

From the above subset definitions and set covers of Ω, application of the usual sub-

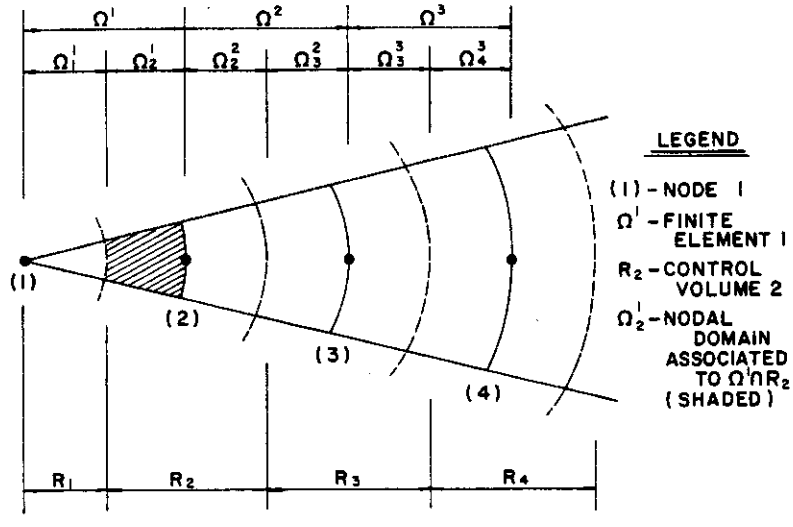

Fig. 1 Nodal domain geometry.

domain method to the governing partial differential operation of Eq. (2) is accomplished by integration of the governing equations over the nodal domains inside each finite element, resulting in a finite-element matrix system similar to that determined by the Galerkin finite-element method.

In this section the governing heat flow equation is integrated over the several nodal domains associated with finite element Ω^e. This approach is simply the subdomain-integration weighted-residual method as applied to a subdomain or control volume, except that the approximation error is averaged over the nodal domains inside the subdomain. These nodal domain contributions can then be reassembled into matrix form for each element Ω^e. Using the previous set notation, the operator relationship for the radially symmetric heat-conduction model of Eq. (1) is

$$A(\phi) - f = \frac{\partial}{\partial R}\left(RK\frac{\partial \phi}{\partial R}\right) - RS\frac{\partial \phi}{\partial t} \tag{17}$$

Substituting Eq. (17) into Eq. (16) gives an element matrix system for Ω^e:

$$\int_{\Omega_f}\left[\frac{\partial}{\partial R}\left(RK\frac{\partial \phi}{\partial R}\right) - RS\frac{\partial \phi}{\partial t}\right] dA = \{0\} \qquad j \in S_e \tag{18}$$

Expanding Eq. (18)

$$\left[\int_{\Gamma_f \cap \Gamma^e}\left(RK\frac{\partial \phi}{\partial n}\right)\Bigg|_{\Gamma_f} ds\right] + \left[\int_{\Gamma_f - \Gamma_f \cap \Gamma^e}\left(RK\frac{\partial \phi}{\partial n}\right)\Bigg|_{\Gamma_f} ds\right] = \int_{\Omega_f} RS\frac{\partial \phi}{\partial t} dA \qquad j \in S_e \tag{19}$$

where the first term of Eq. (19) cancels due to flux contributions from contiguous finite elements or satisfies Neumann boundary conditions on the global boundary Γ, and where (n, s) are normal and tangential vector components on B_j, Γ_f^e, and Γ^e.

To evaluate the integration expressions of Eq. (19), definitions of the finite-element and subdomain covers of global domain Ω are necessary. The finite-element cover Ω^e of Ω is assumed defined by

$$\begin{aligned}
\Omega^1 &\equiv \{(x, y) | 0 = r_1 \le R \le r_2\} \\
\Omega^2 &\equiv \{(x, y) | r_2 \le R \le r_3\} \\
&\cdot \\
&\cdot \\
&\cdot \\
\Omega^{n-1} &\equiv \{(x, y) | r_{n-1} \le R \le r_n = L\}
\end{aligned} \tag{20}$$

where r_i is the radial coordinate of node i; and

$$\Omega \equiv \{(x, y) | 0 \leq R \leq L\}$$

The subdomain cover R_j of Ω is assumed defined by

$$\begin{aligned} R_1 &\equiv \{(x, y) | 0 = 2r_1 \leq 2R \leq (r_1 + r_2)\} \\ R_2 &\equiv \{(x, y) | (r_1 + r_2) \leq 2R \leq (r_2 + r_3)\} \\ &\cdot \\ &\cdot \\ &\cdot \\ R_n &\equiv \{(x, y) | (r_{n-1} + r_n) \leq 2R \leq 2L\} \end{aligned} \tag{21}$$

Therefore, the nodal domain cover Ω_j^e of finite element Ω^e is defined by

$$\Omega^e = \Omega_e^e \cup \Omega_{e+1}^e \tag{22}$$

where (Fig. 1)

$$\begin{aligned} \Omega_e^e &\equiv \frac{(x, y) | r_e \leq R \leq (r_e + r_{e+1})}{2} \\ \Omega_{e+1}^e &\equiv \frac{(x, y) | (r_e + r_{e+1})}{2 \leq R \leq r_{e+1}} \end{aligned} \tag{23}$$

Integration of the governing flow equation on each Ω_j^e involves the definition and integration of the thermal conductivity, K. An approach to handling the nonlinearity problem is to approximately linearize the governing flow equation by assuming the various parameters to be constant for small time steps Δt. For K set to a quasi-constant value K^e in Ω^e during time step Δt, Eq. (19) may be rewritten for the nodal domain Ω_j^e contribution to subdomain R_j as

$$\int_{\Gamma_j - \Gamma_j \cap \Gamma^e} \left(RK^e \frac{\partial \phi}{\partial n} \right) \Bigg|_{\Gamma_j} ds = \int_{\Omega_j} RS \frac{\partial \phi}{\partial t} \, dA \qquad j \in S_e \tag{24}$$

Since the governing heat-flow equation is radially symmetric, Eq. (24) simplifies to (see Fig. 2)

$$\left(RK^e \frac{\partial \phi}{\partial R} \right) \Bigg|_{\Gamma_j - \Gamma_j \cap \Gamma^e} = \int_{\Omega_j} RS \frac{\partial \phi}{\partial t} \, dR \qquad j \in S_e \tag{25}$$

This integrated relationship will be used to develop a subdomain integration model in the following section.

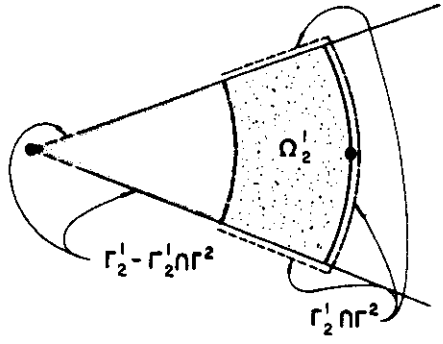

Fig. 2 NDI boundary definitions.

NUMERICAL SOLUTIONS

In the derivation of the finite-element integration statement of Eq. (25) for Ω^e, no specification of the character of the state variable is assumed. In the following, the state variable ϕ is assumed to be adequately approximated by linear trial function ϕ^e in each finite element Ω^e. Therefore it is assumed that $\phi \simeq \phi^e = \Sigma L_j \phi_j^e$ in each Ω^e, where the L_j are the usual linear local coordinates in Ω^e and ϕ_j^e are nodal point values of the temperature trial function estimate in Ω^e. Because of the linear definition of ϕ^e in Ω^e, all spatial gradients of ϕ^e are constant. Consequently, several well-known domain numerical solutions of Eq. (1) in Ω embodied in the finite-element method of weighted residuals result in similar numerical approximations of Eq. (1) in each Ω^e. To develop these domain numerical solutions, the following description variable is defined:

$$\Phi \equiv \frac{\partial}{\partial R}\left(RK\frac{\partial \phi}{\partial R}\right) - RS\frac{\partial \phi}{\partial t} \tag{26}$$

Although the Galerkin method of weighted residuals used to solve Eq. (1) in each Ω^e is well known, its derivation of a finite-element matrix system is presented in order to develop some of the notation and simplifications used in the subsequent determinations of the subdomain integration and integrated finite-difference analogs and to demonstrate the use of flux-type boundary conditions on global boundary Γ.

Galerkin Method of Weighted Residuals

In Ω^e,

$$\int_{\Omega^e} \Phi L_j \, dR \equiv 0 \tag{27}$$

generates a Galerkin finite-element matrix system for approximation of Eq. (1) on Ω^e.

Integrating by parts reduces Eq. (27) to

$$\int_{\Omega^e} \Phi L_j \, dR = RK \frac{\partial \phi}{\partial R} L_j \Big|_{\Gamma^e} - \int_{\Omega^e} \left(RK \frac{\partial \phi}{\partial R} \frac{dL_j}{dR} + SR \frac{\partial \phi}{\partial t} L_j \right) dR \tag{28}$$

The first term in the expansion of Eq. (28) satisfies flux continuity between finite elements and Neumann boundary conditions on global boundary Γ in a manner similar to the NDI statement of Eq. (19).

For $(\phi,K) \equiv (\phi^e,K^e)$ in Ω^e during a small timestep Δt, where ϕ^e is an assumed linear trial function for ϕ in Ω^e, Eq. (28) simplifies to the Galerkin finite-element statement

$$0 \equiv K^e \frac{\partial \phi^e}{\partial R} \int_{\Omega^e} R \frac{dL_j}{dR} \, dR + S \frac{\partial}{\partial t} \int_{\Omega^e} R \phi^e L_j \, dR \tag{29}$$

where

$$K^e \frac{\partial \phi^e}{\partial R} \equiv K^e \left(\frac{\phi_{e+1} - \phi_e}{r_{e+1} - r_e} \right) \tag{30}$$

Integrating Eq. (29) determines the Galerkin finite-element matrix system for the approximation of Eq. (1) on Ω^e:

$$\mathbf{S}^e \boldsymbol{\phi}^e + \mathbf{p}^e(2)\dot{\boldsymbol{\phi}}^e + \mathbf{Q}^e(2)\dot{\boldsymbol{\phi}}^e \equiv \{0\} \tag{31}$$

where

$$\mathbf{S}^e \equiv \frac{K^e}{2l^e}(r_e + r_{e+1}) \begin{bmatrix} 1 & -1 \\ -1 & 1 \end{bmatrix} \tag{32}$$

$$\mathbf{p}^e(2) \equiv \frac{S_e l^e}{6} \begin{bmatrix} 2 & 1 \\ 1 & 2 \end{bmatrix} \tag{33}$$

$$\mathbf{Q}^e(2) \equiv \frac{S(l^e)^2}{12} \begin{bmatrix} 1 & 1 \\ 1 & 3 \end{bmatrix} \tag{34}$$

and where $l^e \equiv (r_{e+1} - r_e)$; and $(\boldsymbol{\phi}^e, \dot{\boldsymbol{\phi}}^e)$ are vectors of the nodal values and time derivative of nodel values of finite element e.

Subdomain Integration

A cover of finite element Ω^e is given by the union of nodal domains Ω_j^e, $j \in S_e$. The subdomain integration version of the weighted-residuals process approximates Eq. (1) in each subdomain R_j by

$$\int_{R_j} \Phi W_j \, dR \equiv 0 \tag{35}$$

where

$$W_j \equiv \begin{cases} 1, R \in R_j \\ 0, \text{otherwise} \end{cases} \tag{36}$$

But

$$\int_{R_j} \Phi W_m \, dR = \int_{\Omega_j} \Phi \, dR + \int_{\Omega_j^{-1}} \Phi \, dR \tag{37}$$

Thus a finite-element matrix system is generated by the subdomain integration method for finite element Ω^e by

$$\int_{\Omega_j} \Phi \, dR \equiv \{0\} \qquad j \in S_e \tag{38}$$

From Eq. (25),

$$\int_{\Omega_j} \Phi \, dR = \left(RK \frac{\partial \phi}{\partial R} \right) \Big|_{\Gamma_j - \Gamma_j \cap \Gamma^e} - \int_{\Omega_j} RS \frac{\partial \phi}{\partial t} \, dR \qquad j \in S_e \tag{39}$$

Using $(K, \phi) \equiv (K^e, \phi^e)$,

$$\int_{\Omega_j} \Phi \, dR \equiv \left(K^e \frac{\partial \phi^e}{\partial R} \right) R \Big|_{\Gamma_j - \Gamma_j \cap \Gamma_j} - S \frac{\partial}{\partial t} \int_{\Omega_j} R \phi^e \, dR \qquad j \in S_e \tag{40}$$

Integrating Eq. (40) gives the finite-element statement of a subdomain integration approximation of Eq. (1) on finite element Ω^e,

$$\mathbf{S}^e \boldsymbol{\phi}^e + \mathbf{p}^e(3) \dot{\boldsymbol{\phi}}^e + \mathbf{Q}^e(3) \dot{\boldsymbol{\phi}}^e \equiv \{0\} \tag{41}$$

where $\mathbf{S}^e$ is given by the Galerkin element matrix of Eq. (32), and

$$\mathbf{p}^e(3) \equiv \frac{S_e l^e}{8} \begin{bmatrix} 3 & 1 \\ 1 & 3 \end{bmatrix} \tag{42}$$

$$\mathbf{Q}^e(3) \equiv \frac{S(l^e)^2}{24} \begin{bmatrix} 2 & 1 \\ 2 & 7 \end{bmatrix} \tag{43}$$

and where vectors $(\boldsymbol{\phi}^e, \dot{\boldsymbol{\phi}}^e)$ are as defined previously.

From Eq. (40), the global finite-element matrix system determined by the appropriate summation of each Ω^e matrix system satisfies Dirichlet and Neumann boundary conditions in a manner similar to the global Galerkin matrix system.

Additionally, the capability of representing an inhomogeneous medium by specifying different parameters in each finite element Ω^e is similar to the usual Galerkin finite-element approach, although from Eq. (40) the conduction parameters are necessarily evaluated at the midpoint of the finite-element and capacitance parameters need to represent a mean value in the control volume associated with the particular nodal point. These advantages normally associated with the Galerkin finite-element approach can also be developed for an integrated finite-difference numerical analog for the approximation of Eq. (1) on Ω^e.

Integrated Finite Difference

The integrated finite-difference approach [3] can be extended to the solution of Eq. (1) on appropriately defined control volumes. The usual control-volume definition, however, is identical to the subdomain definition cover R_j of global domain Ω given by Eq. (21). Thus, an integrated finite-difference approximation for solution of Eq. (1) on Ω^e where the trial function ϕ^e is assumed to be linear in each Ω^e is given by

$$\left(K^e \frac{\partial \phi^e}{\partial R}\right) R\Big|_{\Gamma_j^e - \Gamma_j^e \cap \Gamma^e} = S \frac{\partial}{\partial t} \int_{\Omega_j^e} R\, \phi^e \, dR \qquad j \in S_e \tag{44}$$

But the integrated finite-difference approach equates

$$\int_{\Omega_j^e} \phi^e \, dR \equiv \phi_j \int_{\Omega_j^e} dR \tag{45}$$

Thus, the finite-element matrix system is given by

$$\mathbf{S}^e \boldsymbol{\phi}^e + \mathbf{p}^e(\infty)\dot{\boldsymbol{\phi}}^e + \mathbf{Q}^e(\infty)\dot{\boldsymbol{\phi}}^e \equiv \{0\} \tag{46}$$

where $\mathbf{S}^e$ is once more given by Eq. (32), and

$$\mathbf{p}^e(\infty) \equiv \frac{S_e l^e}{2} \begin{bmatrix} 1 & 0 \\ 0 & 1 \end{bmatrix} \tag{47}$$

$$\mathbf{Q}^e(\infty) \equiv \frac{S(l^e)^2}{8} \begin{bmatrix} 1 & 0 \\ 0 & 3 \end{bmatrix} \tag{48}$$

From Eq. (40), the global finite-element matrix system determined by the appropriate summation of each Ω^e matrix system of Eq. (46) satisfies Neumann and Dirichlet boundary conditions in a manner generally associated with the Galerkin approach. Additionally, anisotropic inhomogeneous mediums are similarly accommodated as with a Galerkin or a subdomain-integration analog previously derived.

Because of the similarity of the three numerical approximations, a single-element matrix system for the approximation of Eq. (1) on Ω^e can be written by

$$\mathbf{S}^e\boldsymbol{\phi}^e + \mathbf{p}^e(\eta)\,\dot{\boldsymbol{\phi}}^e + \mathbf{Q}^e(\eta)\dot{\boldsymbol{\phi}}^e = \{0\} \tag{49}$$

where $\mathbf{S}^e$ is given by Eq. (32); and

$$\mathbf{p}^e(\eta) \equiv \frac{S_e l^e}{2(\eta + 1)}\begin{bmatrix}\eta & 1\\ 1 & \eta\end{bmatrix} \tag{50}$$

$$\mathbf{Q}^e(\eta) \equiv \frac{S(l^e)^2}{4(2\eta^2 - \eta + 3)}\begin{bmatrix}(\eta^2 - 2\eta + 3) & 3\\ (3\eta - 3) & (3\eta^2 - 3\eta + 3)\end{bmatrix} \tag{51}$$

The Galerkin finite-element, subdomain-integration, and integrated finite-difference numerical analogs of Eqs. (31), (41), and (46) are given by Eq. (49) for $\eta = (2, 3, \infty)$, respectively.

Extension of the NDI technique to cylindrical coordinates follows directly from Eqs. (32), (50), and (51). The extension to spherical coordinates follows from the tetrahedral finite-element determination [4] and the above results.

NODAL DOMAIN INTEGRATION MODEL ANALYSIS

The previous section unified several numerical techniques into a single finite-element matrix system as a function of the degree of mass lumping, η. The question remains whether an optimum η factor exists such that the modeling integrated relative error is a minimum.

In this paper the η factor developed for one-dimensional diffusion problems [4] is used to test the NDI model accuracy for radial problems where analytical solutions exist. This technique is based on the Fourier series expansion of a particular solution to the one-dimensional diffusion equation in a small homogeneous control volume. That is, the radial geometric contributions are neglected in the development of η.

For a control volume R_j, the usual process of normalization reduces the one-dimensional diffusion equation to

$$\frac{\partial^2\theta}{\partial x^2} = \frac{\partial\theta}{\partial t} \qquad x \in [0, 1] \tag{52}$$

where θ is a normalized variable for ϕ, and variables x, t are now defined as normalized space and time. It is assumed in Eq. (52) that $\theta(x = 0) = \theta_{j-1}$, $\theta(x = 0.5) = \theta_j$, and $\theta(x = 1) = \theta_{j+1}$, where θ_k are normalized nodal values.

Using the Crank-Nicolson mid-timestep advancement procedure to approximate the time derivative, the nodal equation for solution of θ_j is

$$\frac{\Delta t}{2\|R_j\|}\left[\left(\theta_{j-1}^{i+1} - 2\theta_j^{i+1} + \theta_{j+1}^{i+1}\right) + \left(\theta_{j-1}^{i} - 2\theta_j^{i} + \theta_{j+1}^{i}\right)\right]$$

$$= \frac{\|R_j\|}{2(\eta_j + 1)}\left[\left(\theta_{j-1}^{i+1} - \theta_{j-1}^{i}\right) + 2\eta_j\left(\theta_j^{i+1} - \theta_j^{i}\right) + \left(\theta_{j+1}^{i+1} - \theta_{j+1}^{i}\right)\right] \tag{53}$$

where the normalized length $\|R_j\| = \frac{1}{2}$; i is the timestep number; and η_j is constant during normalized timestep Δt. Equation (53) evaluates all modeled flux terms at the mid-timestep. For other time-derivative approximations, such as forward or backward step differencing, a similar difference statement can be developed. A solution of Eq. (52) using Eq. (53) at the mid-timestep is

$$\hat{\theta}(x, \epsilon) = -\frac{1}{2}(\bar{\theta}_{j-1} - 2\bar{\theta}_j + \bar{\theta}_{j+1}) \sin \pi x e^{-\pi^2 \epsilon} + (\bar{\theta}_{j+1} + \bar{\theta}_{j-1})\, x + \bar{\theta}_{j-1} \tag{54}$$

where ϵ is normalized time measured from the mid-timestep; and where $\bar{\theta} = 1/2\,(\theta_j^i + \theta_j^{i+1})$. If it is assumed that all effects of a moving boundary value at the endpoints is equivalent to holding θ constant at the mid-timestep boundary values, then Eq. (54) represents an exact solution to the assumed boundary-value problem.

Holding the boundary values of $\hat{\theta}$ constant at the mid-timestep allows a simplification of the NDI nodal equation to

$$\frac{\Delta t}{\|R_j\|}\left[\left(\bar{\theta}_{j-1} + \bar{\theta}_{j+1}\right) - \left(\theta_j^i + \theta_j^{i+1}\right)\right] = \frac{\|R_j\|}{2(\eta_j + 1)}\left[2\eta_j\left(\theta_j^{i+1} - \theta_j^i\right)\right] \tag{55}$$

Solving for θ_j^i and θ_j^{i+1} gives

$$\theta_j^i = \hat{\theta}\left(\frac{1}{2}, \frac{-\Delta t}{2}\right) = -\frac{1}{2}\left(\bar{\theta}_{j-1} - 2\bar{\theta}_j + \bar{\theta}_{j+1}\right)e^{\pi^2 \Delta t/2} + \frac{1}{2}\left(\bar{\theta}_{j-1} + \bar{\theta}_{j+1}\right) \tag{56a}$$

$$\theta_j^{i+1} = \hat{\theta}\left(\frac{1}{2}, \frac{\Delta t}{2}\right) = -\frac{1}{2}\left(\bar{\theta}_{j-1} - 2\bar{\theta}_j + \bar{\theta}_{j+1}\right)e^{-\pi^2 \Delta t/2} + \frac{1}{2}\left(\bar{\theta}_{j-1} + \bar{\theta}_{j+1}\right) \tag{56b}$$

Combining Eqs. (56*a*), (56*b*), and (55) gives η_j as a function of the model timestep size by

$$\eta_j(\Delta t) = \frac{4\,\Delta t(1 + e^{-\pi^2 \Delta t})}{1 - e^{-\pi^2 \Delta t} - 4\,\Delta t(1 + e^{-\pi^2 \Delta t})} \tag{57}$$

where the normalized timestep Δt is related to the global model timestep Δt^* by

$$\Delta t = \frac{\Delta t^*}{4\mathcal{D}\|R_j\|^2} \tag{58}$$

where $\mathcal{D}$ is the mean diffusivity ($\mathcal{D} = K/S$) for R_j. From Eq. (57), the mass lumping factor lies within the range

$$\frac{8}{\pi^2 - 8} \leq \eta_j(\Delta t) < \infty \tag{59}$$

and is seen to be a function of timestep and element size.

To test the success of the $\eta(\Delta t)$ selection technique, several radially symmetric heat transfer (diffusion) problems where analytic solutions are known were modeled. Additionally, the derived η factors of 2, 3, and ∞ were also tested for comparison purposes. The measure of accuracy used is a form of the L_2 norm of the error given by

$$E = \frac{\left[\int_\Omega (\phi - \hat{\phi})^2 \, d\Omega\right]^{1/2}}{\int_\Omega d\Omega} \tag{60}$$

where ϕ is the test problem solution; $\hat{\phi}$ is the approximation value, and E is the error of approximation.

In this study, six different boundary-value problems of the heat flow equation were tested with various values of the timestep (Crank-Nicolson method) and finite-element size. For each test, nodal values are reset to the exact nodal values after each timestep advancement in order to better test the approximation error in satisfying the flow equation rather than measuring the accumulation of approximation error. After each timestep, the E error is evaluated and stored for the four considered η factor approaches, and the factor that results in the minimum E value (a success) is noted. Consequently, more than 150 test problems (five timesteps and five element spacings for each boundary-value problem) resulted in an excess of 20,000 timestep advancements. By dividing the number of successes by the total number of timestep advancements, a probability of success for a η factor is estimated. Figure 3 shows the success probability for the $\eta(\Delta t)$ approach as a function of normalized timestep size and element size.

It is noted that the redefinition of nodal values to the exact nodal values (obtained from the analytic solution) eliminates the bias in accumulative numerical error due to a large deviation in any one timestep. Because all the mass-lumped values provide for a stable and convergent domain numerical technique, the significance in varying the matrix mass lumping is made apparent in the success of each timestep advancement. Figure 3 demonstrates empirical evidence that the proposed mass-lumping scheme of Eq. (57) provides for significant increase in modeling accuracy over each timestep as compared to the other mass-lumped schemes of finite difference and finite element.

For larger normalized timesteps (greater than 0.025), all the numerical techniques considered showed similar rates of success and failure in achieving the best results. Each of the models produced relatively poor results for such large timesteps and would generally not be used in modeling transient heat flow problems.

CONCLUSIONS

A unifying numerical model can be developed for radially symmetric heat conduction problems. The unifying model is based on the straightforward nodal domain integration method. The resulting model is found to have the capability of repre-

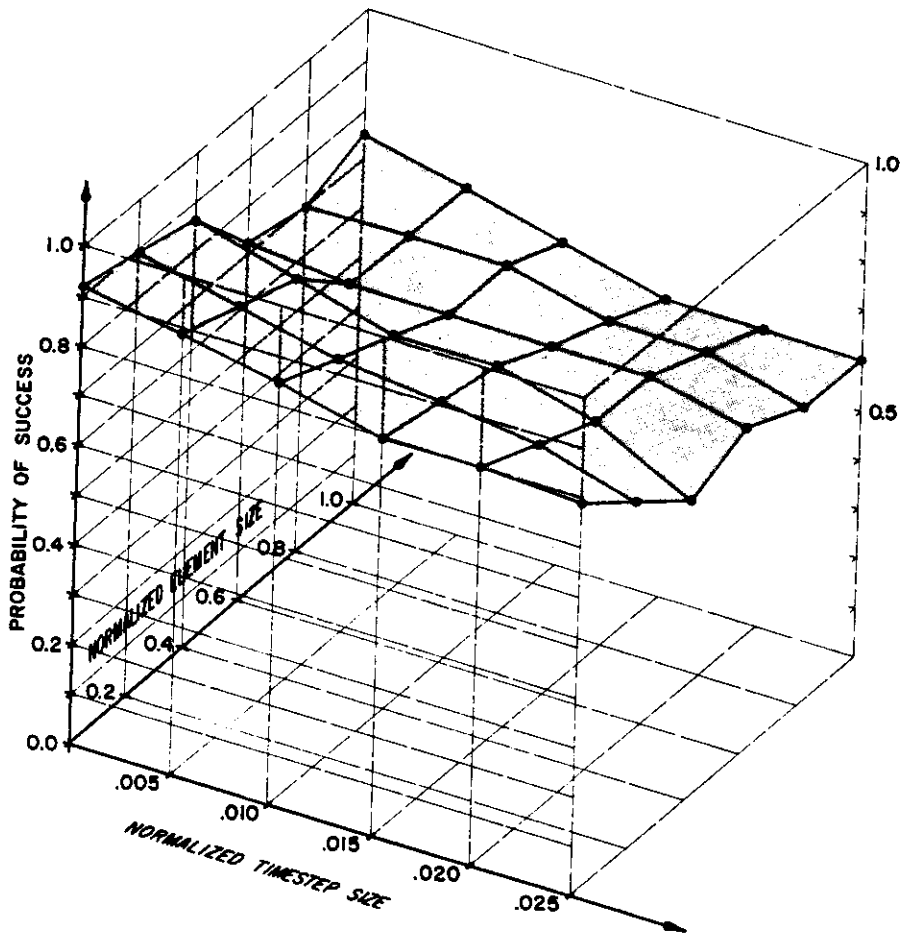

Fig. 3 Probability of success using Eq. (57).

senting the Galerkin finite-element, subdomain-integration, and integrated finite-difference methods by the specification of a single mass matrix lumping factor η.

The global matrix system composed of the sum of all NDI elements accommodates Dirichlet, Neumann, and mixed boundary conditions without the need for special finite-differencing equations.

An infinity of possible domain numerical methods are possible and can be represented by the NDI model for specific values of η.

A computer code based on the Galerkin finite-element method can easily be modified to allow a variable mass lumped matrix system and, consequently, represent an integrated finite-difference, subdomain-integration, and an infinity of other domain methods.

An improved mass lumping factor exists (as a function of timestep and finite-element size) that minimizes approximation error more often than any of the other domain methods considered. The probability of the proposed optimum mass-lumping system being the best numerical method is approximately 70% for the normalized

timestep sizes considered. The improved method is developed based on a linear trial function model and a Crank Nicolson time advancement approximation. Although only the radially symmetric problem is developed, the extension of the approach to cylindrical and spherical coordinate problems is straightforward.

REFERENCES

1. T. V. Hromadka II and G. L. Guymon, Mass Lumping Models of Three-dimensional Heat Conduction, *Num. Heat Transfer*, vol. 6, no. 3, 1983.
2. O. C. Zienkiewicz, *The Finite Element Method in Engineering Science*, McGraw-Hill, New York, 1977.
3. D. B. Spalding, A Novel Finite-Difference Formulation for Differential Expressions Involving Both First and Second Derivations, *Int. J. Numer. Meth. Eng.*, vol. 4, p. 551, 1972.
4. T. V. Hromadka II and G. L. Guymon, Mass Lumping Models of the Linear Diffusion Equation, *Adv. Water Resources*, vol. 6, pp. 79–87, 1983.

Received April 23, 1984
Accepted February 4, 1985

Requests for reprints should be sent to T. V. Hromadka II.